

Effects of surface etching on microstructure and mechanical strength of carbon fibers

Kwan-Woo Kim^{1,2}, Jin-Soo Jeong^{2,3}, Dong Chul Chung¹, Kay-Hyeok An^{3,*}, and Byung-Joo Kim^{1,3,*}

¹Research Laboratory for Multifunctional Carbon Materials, Korea Institute of Carbon Convergence Technology, Jeonju 54853, Republic of Korea

²Department of Organic Materials & Fiber Engineering, Chonbuk National University, Jeonju 54896, Republic of Korea

³Department of Carbon and Nano Materials Engineering, Jeonju University, Jeonju 55069, Korea

Key words: carbon fiber, surface, etching, tensile strength, microstructure

Article Info

Received 20 February 2018

Accepted 17 March 2018

*Corresponding Author

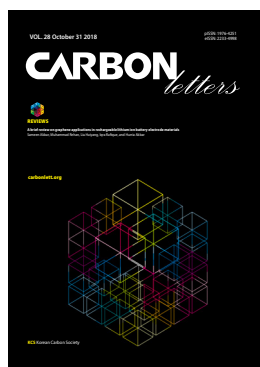
E-mail: kimbj2015@gmail.com
khan@jj.ac.kr

Tel: +82-63-219-3710
+82-63-220-2228

Open Access

DOI: <http://dx.doi.org/10.5714/CL.2018.28.100>

This is an Open Access article distributed under the terms of the Creative Commons Attribution Non-Commercial License (<http://creativecommons.org/licenses/by-nc/3.0/>) which permits unrestricted non-commercial use, distribution, and reproduction in any medium, provided the original work is properly cited.



<http://carbonlett.org>

pISSN: 1976-4251
eISSN: 2233-4998

Copyright © Korean Carbon Society

Carbon fiber (CF) is recognized as an optimal reinforcement for the composites application areas which light weight and high mechanical properties are needed [1,5,11]. The use of CFs are increasing in the fields of military, aerospace, ship building, and sports goods due to these reasons. Additionally, the applications of CFs are becoming wider to the automobile industries. And it is even accelerating by the development of low cost and high performance CFs [1,2,5]. CFs can be classified by the origins of precursors. There are representatively polyacrylonitrile (PAN)-based, pitch-based and rayon-based fibers, but it is well recognized that PAN-based CFs have high mechanical properties [9]. Typical properties of PAN-based CFs are known as high tensile strength and modulus. These features are due to the ribbon-like microstructure in the fiber, and it is reported to cause the high performance of the fiber [3,8,10].

For the application of military industries, CFs are normally used as a reinforced material for structural parts. In this case, the natural properties of CFs are thinkable more important than other application areas such as sports goods and automobile industries. In order to obtain proper features of CFs, the design of manufacturing process for CFs is very crucial to determine the mechanical properties including tensile strength & modulus, elongation, and so on [3,4,6].

It is known that the production process of PAN-based CF has the basic processes such as polymerization, spinning, stretching, stabilization, carbonization and surface treatment, and that the mechanical strength of PAN fiber depends heavily on the composition of each process step [7,13]. A better PAN precursor requires relatively small diameters, high molecular orientation in the fiber axis direction, high crystallinity, and low activation energy for the cyclization reaction [28].

The spinning process includes wet spinning, melt-assisted spinning (a process in which the highly concentrated polymer solution is heated under pressure and then the solvent is removed from the spinning chamber), and dry-wet spinning (a method of spinning with a short air-gap layer so as to be molecular orientation), and the spinning process plays absolutely a key role in the molecular orientation of the precursor fibers [14,19,20].

The PAN fiber produced by the spinning process is stabilized (the process of making the stable precursor by cyclization through oxidation at a temperature of 300°C. The fiber density is round 1.30 to 1.40 g/cc) and then carbonized at 1200°C (the carbon content is increased to 90% or more. The final density of the fiber is around 1.6 to 1.8 g/cc), and finally, the CF is manufactured [12,15-18,23]

In all manufacturing processes, the surface of the CF is subject to various defects for the following reasons: (1) unevenness of the polymer chain orientation due to friction between the nozzle wall and the PAN resin in the spinning process, (2) unbalance of force applied during stretching and thus surface cracking, (3) uneven reaction with oxygen during stabilization, (4) Surface cracks due to fiber volume shrinkage during carbonization process. These various surface defects of CF remain as obstacles to the development of high

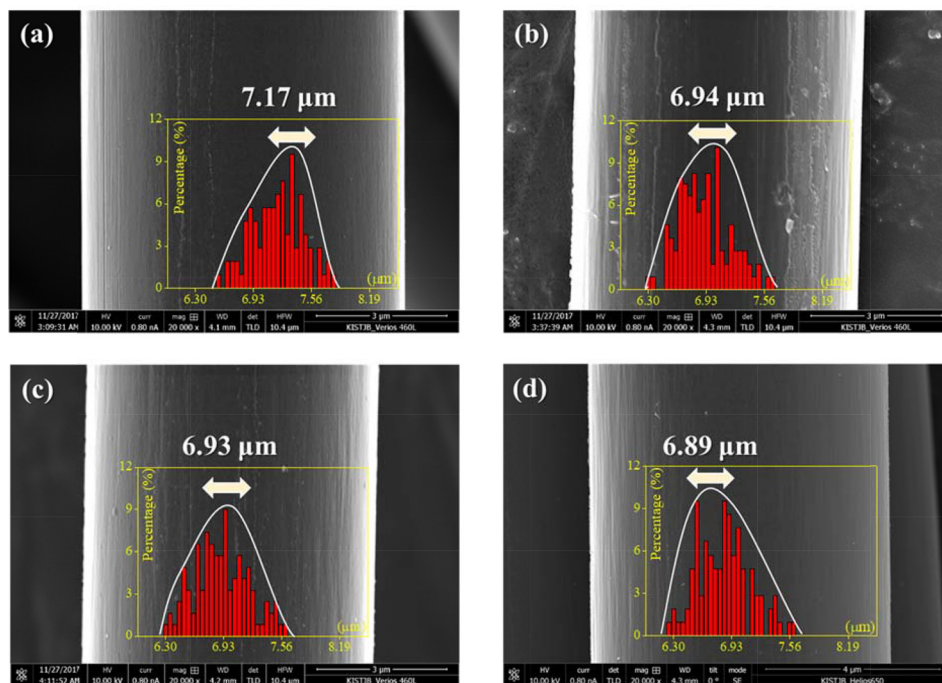


Fig. 1. Scanning electron microscopy micrographs of the carbon fibers (CFs); (a) Virgin CFs (desized), (b) 500-60, (c) 500-120, (d) 500-240. Samples from (b) to (d) were treated by super-heated steam surface modification at 500°C as a function of treatment time from 60 min to 240 min.

performance fibers [21,22,24].

Since the diameter of all industrial fibers is directly related to the mechanical strength of the fiber, recent attempts have been made to reduce the diameter of the CF from 7 μm to 5 μm . Theoretically, it is known that the tensile strength of the CF can be increased by 15% [29].

Wang et al. [30] reported that CFs which were etched by plasma exhibited enhanced crystallinity and tensile modulus with increasing etching depth. And they showed the maximum increase when the etching depth was around 1.1–1.6 μm from the surface. The crystallinity of CFs is observed to be decreased from the core to the surface due to the unevenness of the polymer chain orientation and surface defect caused from spinning and carbonization processes mentioned above. So, it is possible to make a conclusion that the mechanical properties of CFs can be controllable by the degree of etching treatments.

Therefore, as described above, when a technique of successfully removing surface defects present in CFs and simultaneously reducing the diameter of CFs is developed, it is possible to simultaneously control the mechanical strength of the CFs and the surface polarity control.

In the TGA results of the previous study [25], CFs showed a weight loss of less than 5% when heated to 500°C under superheated steam (SHS) conditions. It is considered that the amorphous structure is mainly selectively decomposed [26]. In addition, it was confirmed that the CF can be etched uniformly from the surface of the CF under severe conditions.

In this study, surface defects and surface layer etching of CF were tried using previous research results [25], and the mechanical strength changes of CF according to surface etching were investigated.

The CFs studied in this work were PAN-based unidirectional CFs (T700, Toray Co., Japan). A fixed SiC furnace was used to surface treatment (or etching) the CFs. Alumina tube, with a length of 1000 mm and an inner diameter of 80 mm, was horizontal mounted in an electrical resistance furnace (15 kW) and heated to final temperatures of 500°C and held for 30 to 240 min. A removable porcelain crucible containing the sample was positioned in the centre of the alumina tube. The CFs were heated with 5 °C/min of heating rate from the room temperature in a furnace under steam (liquid flow 2 ml/min) and kept at the target temperature for difference time to obtain SHS surface treated CFs. Then, the gas flow was switched to inert gas (N_2) at a rate of 200 ml/min, SHS surface treated CFs series were obtained after cooling down to room temperature.

The differences in the structure of the CFs treated under different time conditions were determined using a wide-angle X-ray diffractometer (XRD, EMPYREAN, PANalytical, Netherlands), employing a EMPYREAN X-ray diffractor with a customized auto-mount and a $\text{CuK}\alpha$ radiation source at 40 kV and 30 mA. Diffraction patterns were collected within diffraction angles from 10° to 60° with a speed of 2 °/min.

The morphology of the virgin and treated CFs were explored with a field-emission scanning electron microscopy (FE-SEM, NOVA NanoSEM, FEI, Netherlands). In order to reduce charging during scanning electron microscopy imaging, samples were first placed on a sample holder and coated with platinum. The base pressure of the analyzer chamber was about 5×10^{-5} Pa. The acceleration voltage was 10 kV.

Single-fiber tensile tests were performed according to the standard ISO 11566. The mounting specimen was carefully aligned with the loading axis of the universal testing machine

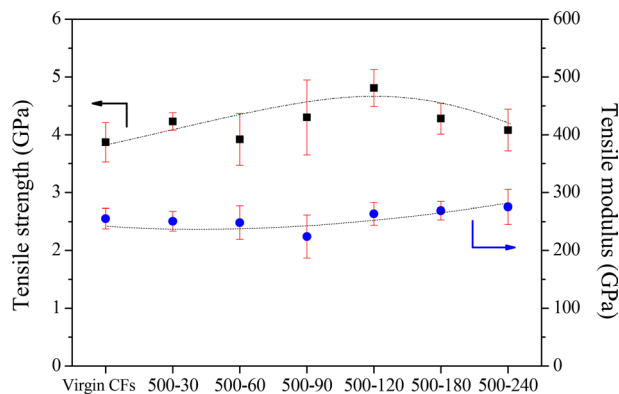


Fig. 2. Single fiber tensile properties of the carbon fibers (CFs). Samples from 500-30 to 500-240 were treated by super-heated steam surface modification at 500°C as a function of treatment time from 30 min to 240 min.

(UTM, Lloyd, UK). The gauge length of the fiber was 20 mm and the draw-off clamp speed was set at 0.3 mm/min. Both sides of the specimen window were cut carefully at the mid-gauge point to leave the filament suspended between the grips of the testing machine. The carbon fiber was loaded until failure, and the force-displacement curve was recorded. At least 60 fibers were tested for each sample.

Figure 1 exhibits the FE-SEM images which shows surface morphologies and diameter changes of SHS-treated CFs as a function of different treatment times.

The surface of virgin CFs was shown to have narrow gaps which generated with fiber axial during the manufacturing process. It was observed that the roughness was changed repeatedly from smooth surface to coarse surface with increasing treatment times. Additionally, fiber diameter decreased overall from around 7.17 μm to 6.89 μm . These results can indicate that the SHS treatment caused the oxidation of amorphous or semi-crystalline structures at first and then etched more enough to show clean surfaces and decreasing in diameter of fibers. It (structural changes) can be thinkable to affect (or increase) the mechanical performance of carbon fibers.

In order to observe mechanical properties of CFs after SHS treatments, a single fiber tensile test was measured and the results exhibited in Figure 2.

All CFs showed higher tensile strength overall than that of the virgin fiber [25]. In case of the '500-120' sample (it means the sample which treated at 500°C for 120 min), the tensile strength and modulus of the fiber increased 24% and 3%, respectively. This is the maximum value of this research.

It is interesting to note that the tensile strength of the fiber exhibited increase and decrease repeatedly. This observation shows good match with SEM images. In SEM images, repetitive changes of surface roughness was observed due to the nonhomogeneous oxidation behaviors, which amorphous domains were oxidized first and then semi-crystalline domains were etched. Therefore, tensile strength can be probably decreased in the step of amorphous oxidation and then be enhanced in the following step of etching, resulting in the repetitive changes of mechanical properties of CFs.

It was also observed that the tensile strength of CFs were

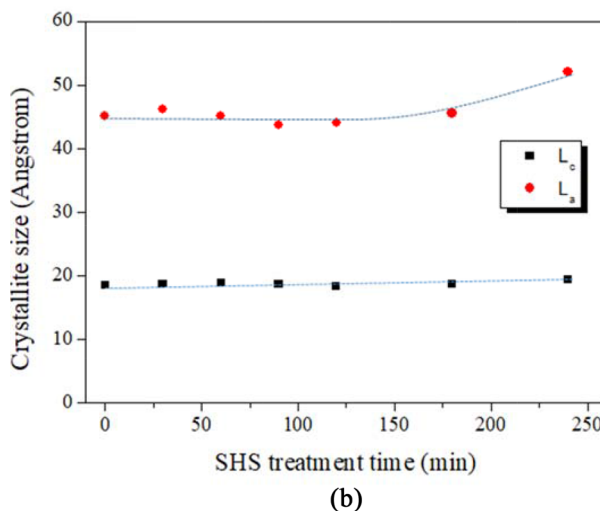
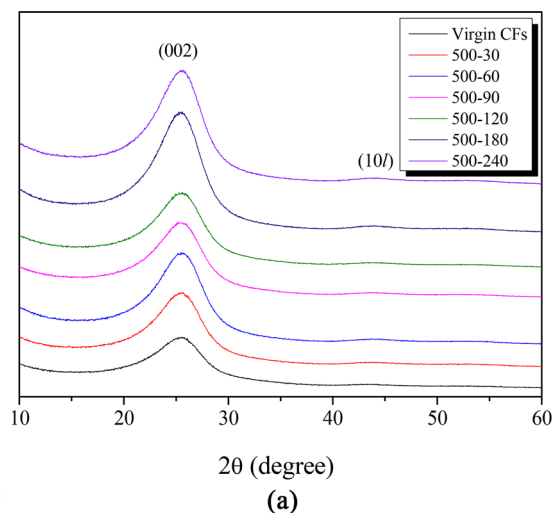


Fig. 3. X-Ray diffraction patterns (a) and crystallite size (b) of the carbon fibers (CFs). Samples from 500-30 to 500-240 were treated by super-heated steam surface modification at 500°C as a function of treatment time from 30 min to 240 min.

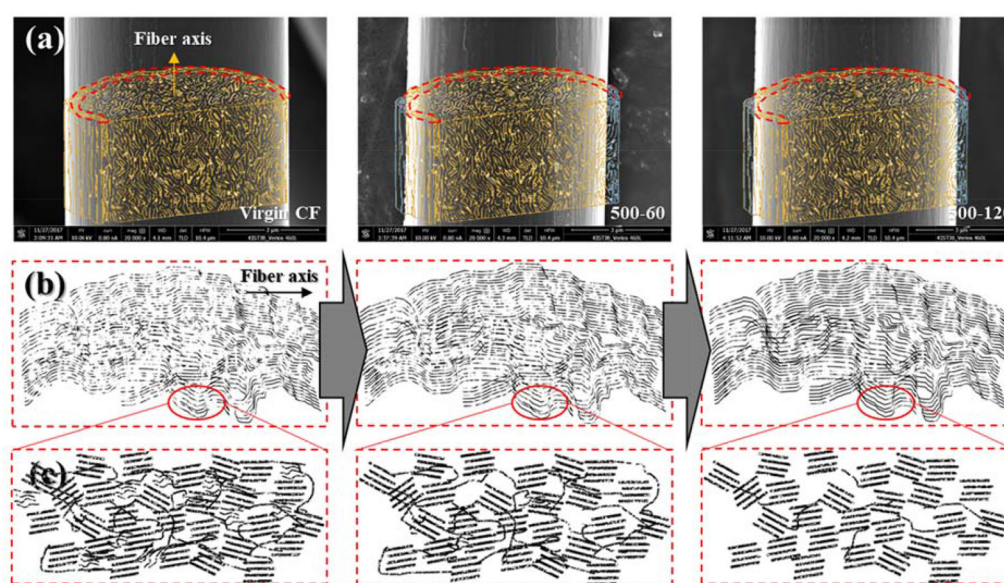
decreased after 180 min of treatment time. This result can be explained that severe oxidation condition led to selective oxidation of overall amorphous domains in the CFs and caused the breaks of stress propagation routes. Meanwhile, tensile modulus of CFs were slightly enhanced probably due to the high degree of graphitic domain after severe oxidation and showed the highest value (275 GPa, 8% of increase compared to virgin CFs) in the '500-240' sample.

XRD analysis was used to observe the structural changes as described above, and the results are shown in Figure 3 and Table 1. All treated CFs showed an increase in the intensity of C(002) peaks compared to that of the virgin CF, of which '500-60' sample showed the highest increase (the FWHM showed the lowest value).

In order to observe the change of the crystal structure in detail, the grain size was analyzed using Scherrer's equation and the results are shown in Table 1.

Table 1. Structural Parameters of the Carbon Fibers and Super-Heated Steam Surface Treated Carbon Fibers.

Sample	002 peak				101 peak			
	2θ	d_{002} (Å)	FWHM (2 θ)	L_c (Å)	2θ	d_{101} (Å)	FWHM (2 θ)	L_a (Å)
Virgin CFs	25.49	3.49	4.39	18.57	43.74	2.07	3.88	45.15
500-30	25.49	3.49	4.39	18.59	43.74	2.07	3.79	46.22
500-60	25.57	3.48	4.31	18.92	43.97	2.06	3.88	45.18
500-90	25.52	3.49	4.35	18.74	43.96	2.06	4.01	43.72
500-120	25.52	3.49	4.43	18.40	43.92	2.06	3.98	44.04
500-180	25.44	3.50	4.36	18.70	43.78	2.07	3.84	45.62
500-240	25.55	3.49	4.36	19.46	43.96	2.06	3.37	52.02

**Fig. 4.** Surface structure change mechanism of the carbon fibers (CFs); (a) Scanning electron microscopy micrographs, (b) texture images, and (c) scheme images. Images from (b) and (c) show the surface structure change of the red dotted line in (a).

In the longitudinal direction (L_c), as the treatment time increased, the L_c size of the CFs did not show a large change within 2% from the initial 18.57 to 18.92. And it was observed that the size did not exhibit the significant changes until 120 min of treatment time and then dramatically enhanced by about 15% in the transverse direction (L_a). Specifically, in the case of longitudinal direction, it was observed that the interplanar spacing was inversely proportional to the front and the rear of '500-60' sample because the amorphous portion existing inside the CF was preferentially decomposed during the SHS treatment to form a vacancy in the structure. It is considered that the interplanar spacing of the fiber might be increased again by the structural densification from the graphite domain reorientation. L_a , as described above, showed a marked increase after 120 minutes because the oxidation (or etching) of the CF occurs gradually as the SHS treatment time is increased. The average crystallite size (it is a statistical size.) was increased probably due to the oxidation of small crystals which can be oxidized

by severe conditions compared to the amorphous domains that oxidized first in the SHS treatment [27]. This excessive oxidation might cause the decrease in diameter of the CFs.

Figure 4 is a schematic diagram showing the change in crystal structure that can be occurred as oxidation progresses outer walls of the CFs.

From the results of SEM and XRD, it has been confirmed that the crystallinity is increased in the statistical aspect by oxidation and structural densification of the amorphous part, and the concept is shown in (b) and (c). In this process, the tensile strength of the CF tended to increase (24% higher than that of the virgin) until 120 minutes of treatment time and then to decrease again. This is equivalent to the point at which the L_a value is greatly increased due to the oxidation of amorphous and small crystals. It has been confirmed that the etching treatment of CFs can absolutely help increase the tensile strength, but excessive oxidation conditions in the crystal structure lead to a decrease in mechanical strength of the CF itself.

Acknowledgments

This study was supported by the “Institute of Civil Military Technology Cooperation (Project No.17-CM-MA-24)” and Industrial Core Technology Development Program (Project No.10083615) funded by the Ministry of Trade, Industry Energy (MOTIE), Republic of Korea.

References

- [1] Herrera-Sosa ML. Valadez-González A. Vázquez-Torres H. Mani-González PG. Herrera-Franco PJ. Effect of the surface modification using MWCNTs with different L/D by two different methods of deposition on the IFSS of single carbon fiber-epoxy resin composite. *Carbon Lett*, **24**, 18 (2017).
- [2] Soutis C. Fiber reinforced composites in aircraft construction. *Prog Aerospace Sci*, **41**, 143 (2005).
- [3] Paiva MC. Bernardo CA. Nardin M. Mechanical, surface and interfacial characterization of pitch and PAN-based carbon fiber. *Carbon*, **38**, 1323 (2000).
- [4] Dai Z. Zhang B. Shi F. Li M. Zhang Z. Gu Y. Chemical interaction between carbon fibers and surface sizing. *App Polym Sci*, **124**, 2127 (2012).
- [5] Oh SM. Lee SM. Kang DS. Roh JS. Microstructural changes of polyacrylonitrile-based carbon fibers (T300 and T700) due to isothermal oxidation (1): focusing on morphological changes using scanning electron microscopy. *Carbon Lett*, **18**, 18 (2016).
- [6] Kim HI. Choi WK. Oh SY. Seo MK. Park SJ. An KH. Lee YS. Kim BJ. Effects of oxyfluorination on surface and mechanical properties of carbon fiber-reinforced polarized-polypropylene matrix composites. *Nanosci Nanotechnol*, **14**, 9097 (2014).
- [7] Maradur SP. Kim CH. Kim SY. Kim BH. Kim WC. Yang KS. Preparation of carbon fibers from a lignin copolymer with polyacrylonitrile. *Synthetic Metals*, **162**, 453 (2012).
- [8] Li W. Long D. Miyawaki J. Qiao W. Ling L. Mochida I. Yoon SH. Structural features of polyacrylonitrile-based carbon fibers. *Mater sci*, **47**, 919 (2012).
- [9] Qin X. Lu Y. Xiao H. Wen Y. Yu T. A comparison of the effect of graphitization on microstructures and properties of polyacrylonitrile and mesophase pitch-based carbon fibers. *Carbon*, **50**, 4459 (2012).
- [10] Edie DD. The effect of processing on the structure and properties of carbon fiber. *Carbon*, **36**, 345 (1998).
- [11] Herrera-Sosa ML. Valadez-González A. Vázquez-Torres H. Mani-González PG. Herrera-Franco PJ. Effect of the surface modification using MWCNTs with different L/D by two different methods of deposition on the IFSS of single carbon fiber-epoxy resin composite. *Carbon Lett*, **24**, 18 (2017).
- [12] Arbab S. Teimoury A. Mirbaha H. Adolphe DC. Noroozi B. Nourpanah P. Optimum stabilization processing parameters for polyacrylonitrile-based carbon nanofibers and their difference with carbon (micro) fiber, **142**, 198 (2017).
- [13] Arshad SN. Naraghi M. Chasiotis I. Strong carbon nanofibers from electrospun polyacrylonitrile, *Carbon*, **49**, 1710 (2011).
- [14] Liu J. Zhou P. Zhang L. Ma Z. Liang J. Fong H. Thermo-chemical reactions occurring during the oxidative stabilization of electrospun polyacrylonitrile precursor nanofibers and the resulting structural conversions. *Carbon*, **47**, 1087 (2009).
- [15] Xie Z. Niu H. Lin T. Continuous polyacrylonitrile nanofiber yarns: preparation and dry-drawing treatment for carbon nanofiber production. *RSC Adv*, **5**, 15147 (2015).
- [16] Wu SH. Qin XH. Effects of the stabilization temperature on the structure and properties of polyacrylonitrile-based stabilized electrospun nanofiber microyarns. *Therm Anal Calorim*, **116**, 303 (2014).
- [17] Cipriani E. Zanetti M. Bracco P. Brunella V. Luda M. Costa L. Crosslinking and carbonization processes in PAN films and nanofibers. *Polym Degrad Stab*, **123**, 178 (2016).
- [18] He JH. Wan YQ. Yu JY. Effect of concentration on electrospun polyacrylonitrile (PAN) nanofibers. *Fibers Polym*, **9**, 140 (2008).
- [19] Lai G. Zhong G. Yue Z. Chen G. Zhang L. Vakili A. Wang Y. Zhu L. Liu J. Fong H. Investigation of post-spinning stretching process on morphological, structural, and mechanical properties of electrospun polyacrylonitrile copolymer nanofibers. *Polymer*, **52**, 519 (2011).
- [20] Sun J. Zhao F. Yao U. Jin Z. Liu X. Huang U. High efficient and continuous surface modification of carbon fibers with improved tensile strength and interfacial adhesion. *Applied Surface Science*, **412**, 424 (2017).
- [21] Vautard F. Dentzer J. Nardin M. Schultz J. Defoort B. Influence of surface defects on the tensile strength of carbon fibers. *Appl Surf Sci*, **322**, 185 (2014).
- [22] Moreton R. Watt W. Tensile strengths of carbon fibres. *Nature*, **247**, 360 (1974).
- [23] Yu W. Yao J. Tensile strength and its variation for PAN-based carbon fibers I. Statistical distribution and volume dependence. *Appl. Polym. Sci*, **101**, 3175 (2006).
- [24] Chae HG. Newcomb BA. Gulgunje PV. Liu Y. Gupa KK. Kamath MG. Lyons KM. Ghoshal S. Pramanik C. Giannuzzi L. Sahin K. Chasiotis I. Kumar S. High strength and high modulus carbon fibers. *Carbon*, **93**, 81 (2015).
- [25] Kim KW. Lee HM. An JH. Chung DC. An KH. Kim BJ. Recycling and characterization of carbon fibers from carbon fiber reinforced epoxy matrix composites by a novel super-heated-steam method. *J Environ Manage*, **203**, 872 (2017).
- [26] Baek J. Lee HM. Roh JS. Lee HS. Kang HS. Kim BJ. Studies on preparation and applications of polymeric precursor-based activated hard carbons: I. Activation mechanism and microstructure analyses. *Microp Mesop Mat*, **219**, 258 (2016).
- [27] Roh JS. Microstructural changes during activation process of isotopic carbon fibers using CO₂ Gas(I)-XRD Study. *Kor J Mater Res*, **13**, 742 (2003).
- [28] Mathur RB. Bahl OP. Mittal J. Advances in the development of high-performance carbon fibres from PAN precursor. *Comp Sci Technol*, **51(2)**, 223 (1993).
- [29] Kobayashi T. Sumiya K. Fukuba Y. Fujie M. Takahagi T. Tashiro K. Structural heterogeneity and stress distribution in carbon fiber monofilament as revealed by synchrotron micro-beam X-ray scattering and micro-Raman spectral measurements. *Carbon*, **49(5)**, 1646 (2011).
- [30] Hao L. Peng P. Yang F. Zhang B. Zhang J. Lu X. Jiao W. Liu W. Wang R. He X. Study of structure-mechanical heterogeneity of polyacrylonitrile-based carbon fiber monofilament by plasma etching-assisted radius profiling. *Carbon*, **114**, 317 (2017).